Methane Steam Reforming, Methanation and Water-Gas Shift: I. Intrinsic Kinetics

Intrinsic rate equations were derived for the steam reforming of methane, accompanied by water-gas shift on a $Ni/MgAl_2O_4$ catalyst. A large number of detailed reaction mechanisms were considered. Thermodynamic analysis helped in reducing the number of possible mechanisms. Twenty one sets of three rate equations were retained and subjected to model discrimination and parameter estimation. The parameter estimates in the best model are statistically significant and thermodynamically consistent.

Jianguo Xu
Gilbert F. Froment
Laboratorium voor
Petrochemische Techniek
Rijksuniversiteit Gent
Gent, Belgium

Introduction

Steam reforming on nickel-alumina catalysts is the main process for the production of hydrogen or synthesis gas. It is a large-scale operation carried out in rows of tubular reactors inserted into a gas-fired furnace. The temperature in the tubes evolves from 675 to 1,000 K, necessitating very high heat fluxes. Combined with a pressure of the order of 30 bar, this leads to severe demands for the tube material. The simulation and design of the tubular reactor requires information on thermodynamics and on the kinetics. Whereas the first aspect is fairly well accounted for in the design, the second is often neglected or reduced to very simple elements. It will be shown in the present paper that several reactions have to be considered for a proper description of the process and that the reaction mechanism has to be investigated in some depth to come to a reasonable description of the kinetics. Also, although it is known that the diffusion limitations are severe, most of the kinetic studies either neglect these or resort to so-called "effective" rate equations which do not explicitly account for the resistance to diffusion. The present paper deals with true, intrinsic kinetics on a $Ni/MgAl_2O_4$–spinel catalyst.

Experimental Study

Equipment and materials

The equipment is classical. The preheater and the tubular reactor are made of HK 40 stainless steel (25–20 Cr—Ni). The reactor tube has an inner diameter of 1.07 cm. A thermocouple is sliding in a central tube of 0.35 cm outer diameter. The reaction zone containing the catalyst and inert solid diluent has a length of 10 cm. It is heated by two heaters, each 5 cm long. Four thermocouples are welded on the external reactor wall. Pure α-alumina spheres are used in the preheating section and the section after the catalyst bed. The latter is diluted with α-alumina spheres of the same diameter. The flows of CH_4 and H_2 are measured by rotameters and that of CO_2 by a mass flow meter. Deionized water is fed through a volumetric pump. The hydrogen and methane used are N40 (99.99% purity) and N35 (99.95%) supplied by L'Air Liquide. Carbon dioxide is N25 (99.5%), also from L'Air Liquide. The back pressure is regulated by a membrane pressure regulator. After condensation of the steam and drying, the effluent gas is directed to two gas chromatographs (GC) or to the gas meter and then to the vent.

One of the gas chromatographs uses hydrogen as the carrier gas. The column, with a length of 15 m, is packed with Porapak Q. The other GC, which uses nitrogen as the carrier gas, is used to detect the concentration of hydrogen. The column is filled with 10 m of Porapak Q and 5 m of Porapak N.

Pretreatment of the catalyst

The catalyst contains 15.2% nickel, supported on magnesium spinel. Its BET-surface area is 58 m^2, the nickel surface area 9.3 m^2/g_{cat} (fresh catalyst) and the void fraction 0.528. The original ring-shaped catalyst with outer diameter of 10 mm is crushed into particles of 0.18–0.25 mm.

The amount of catalyst is 0.4 g, which is mixed with about 8 mL of α-alumina diluent. The reactor is first heated in a hydrogen flow, at about 2 K/minute to about 1,083 K. It is kept at that temperature for 12 hrs, after which the temperature is reduced to 823 K. Upon reaching this temperature the pressure is set to 5 bar and the water feed is switched on. The flow controllers are then adjusted to set the reference conditions for testing the activity for steam reforming: $W/F^{\circ}_{CH_4} = 0.2\ g_{cat} \cdot h/mol_{CH_4}$, molar ratio $H_2O/CH_4 = 5.0$, molar ratio $H_2/CH_4 = 1.25$. The activity of the catalyst drops very rapidly during the first 24 hours, but then much more gradually. The kinetic study, with its specific conditions, is started after some 70 hours on stream, when the deactivation has become so slow that only

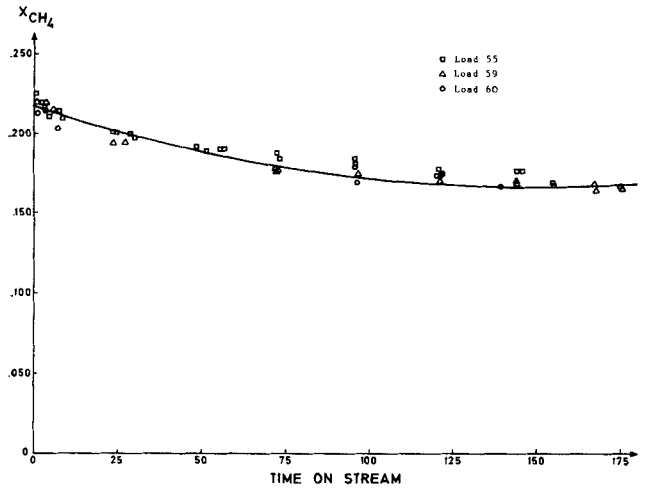

Figure 1. Methane conversion as a function of time at 550°C, p_t = 5 bar, steam to methane molar ratio = 5, hydrogen to methane molar ratio = 1.25, $W/F^o_{CH_4}$ = 0.2 g_{cat} · h/mol CH_4.

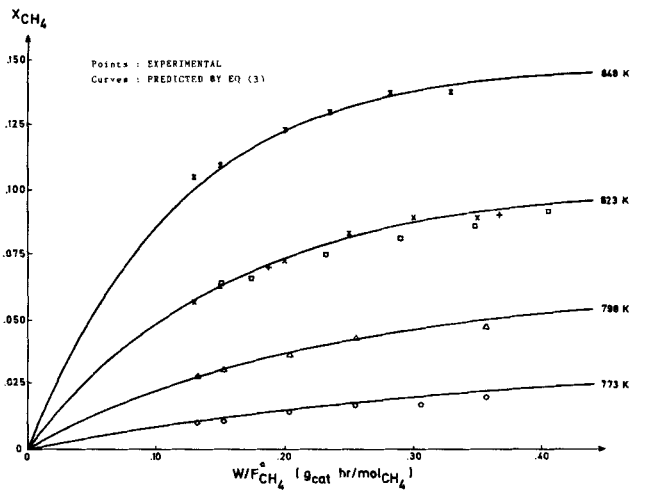

Figure 2. Total conversion of methane vs. space time: $W/F^o_{CH_4}$, p_t = 10 bar, steam to methane molar ratio = 3.

minor corrections, as explained below, are sufficient to account for it. The deactivation is probably caused by sintering.

The pretreatment of fresh catalyst for the experiments on the reverse of the water-gas shift and on the methanation is initially identical to that described above, including the measurement of the reference activity for steam reforming. Then the reference conditions for the reverse of the water-gas shift and methanation are set: T = 673 K; p_t = 3 bar; H_2/CO_2 molar ratio = 1; $W/F^o_{CO_2}$ = 0.25 g_{cat} · h/mol$_{CO_2}$. From then on, there is no more deactivation, except when, under extreme conditions, carbon is accumulating on the catalyst. Because of this, the reference activity level of the reverse of the water-gas shift and methanation is 1.225 times that of steam reforming. This factor is accounted for in the model discrimination and parameter estimation based on the simultaneous treatment of the two sets of experimental results.

Experimental results

A typical methane conversion vs. time on stream behavior is shown in Figure 1. Higher pressures, temperatures, and steam to methane molar ratios increase the deactivation rate. Tests under reference conditions were carried out every day, prior to the runs at other conditions. Because of deactivation, however, the space time required to reach the same conversion as in the first reference test was, say, $(W/F^o_{CH_4})_2$ against $(W/F^o_{CH_4})_1$ in the first test. All the data collected that day were corrected to the reference activity level by multiplying their respective space times with the ratio: $(W/F^o_{CH_4})_1/(W/F^o_{CH_4})_2$.

The conditions covered by the experiments are listed in Table 1. For steam reforming, the temperature range is well below that practiced industrially. Yet, the temperature had to be limited to these values to avoid measuring only equilibrium conversions. Hydrogen was added to the steam reforming feed to avoid reoxidation of the catalyst by steam (De Deken et al., 1982). Figures 2 and 3 show examples of curves of total methane conversion and of conversion of methane into CO_2 vs. $W/F^o_{CH_4}$, experimental and simulated on the basis of rate equations to be presented fur-

Table 1. Experimental Conditions

Pres. bar	H_2O/CH_4 molar	H_2/CH_4 molar	Temp. K
Steam Reforming			
5.0	5.0		
5.0	3.0		
10.0	3.0	1.25	773, 798, 823, 848
15.0	5.0		
3.0	5.0		
3.0	3.0		
Pres. bar		H_2/CO_2 molar	Temp. K
Reverse of Water-Gas Shift and Methanation			
8.0			
10.0		1.0, 0.5	573, 598, 623, 648, 673
3.0			
10.0			

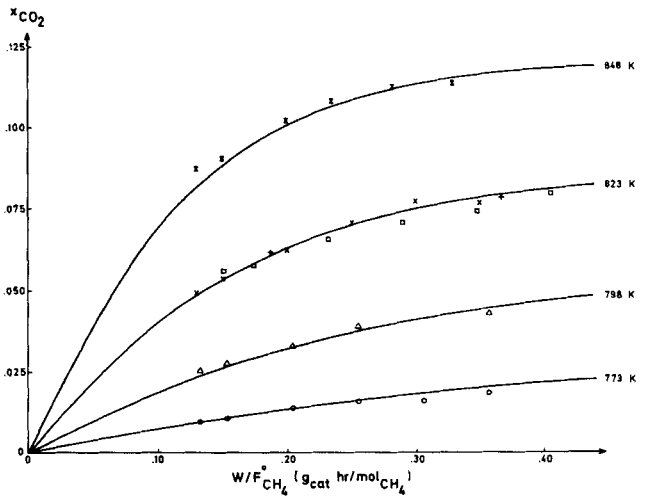

Figure 3. Conversion of methane into CO_2 vs. space time: $W/F^o_{CH_4}$, p_t = 10 bar, steam to methane molar ratio = 3.

ther in this paper. Two hundred and twenty runs were performed on steam reforming.

All the experimental data for the reverse of the water-gas shift and methanation were collected with one load of catalyst, since there was no deactivation. The total CO_2 conversion and the conversion of CO_2 into CH_4 at 10 bar and $H_2/CO_2 = 1$ are plotted in Figures 4 and 5, corrected already for the difference in activity with respect to the steam reforming reference activity level. Sixty runs of this type were performed.

Experiments were carried out with different catalyst sizes for both steam reforming and reverse of the water-gas shift and methanation. It was shown that there were no significant internal diffusion limitations for the size 0.17–0.25 mm. Calculation also proved that external mass and heat transfer resistances were negligible.

Model Development

Thermodynamic analysis

Table 2 lists 11 reactions which may occur, in principle at least, among CH_4, CO_2, CO, H_2, H_2O and carbon. The ratios of

$$\left(\prod_j p_j^{\nu_j}\right)_i \Big/ K_i,$$

represented by $V(i)$, calculated from the experimental results for steam reforming, exceed 1 for the reactions VI–XI, so that no carbon deposition can occur. The values of V(IV) and V(V) are always below 1, so that these two reactions could proceed to the right. Since the observed methane disappearance rate decreased as the methane conversion and therefore the CO_2 concentration increased, in contradiction with IV and V, these reactions were not considered to occur and were left out of the reaction scheme. The ratios V(I) and V(III) monotonously increase with space time, $W/F^{\circ}_{CH_4}$ and temperature, at fixed pressure and steam to methane molar ratio. The values are always smaller than one, so that reactions I and III proceed to the right.

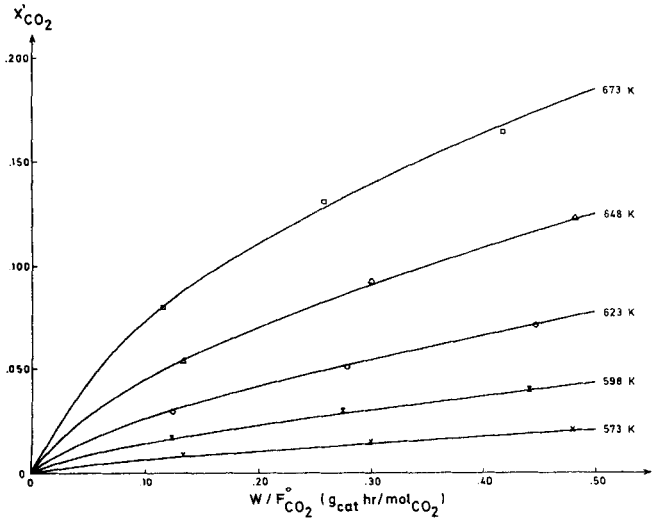

Figure 4. Total conversion of CO_2 vs. space time: $W/F^{\circ}_{CO_2}$, p_t = 10 bar, molar H_2/CO_2 = 1.0.

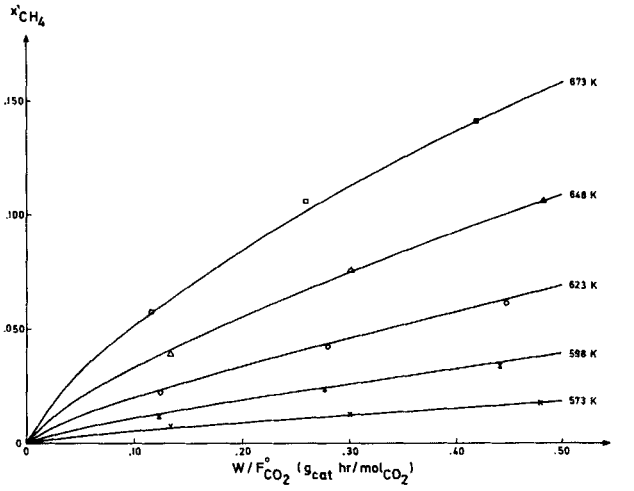

Figure 5. Conversion of CO_2 into methane vs. space time: $W/F^{\circ}_{CO_2}$, p_t = 10 bar, molar H_2/CO_2 = 1.0.

The V(II) values are shown in Figure 6 for various ratios of water to methane, pressures, and temperatures. At 10 to 15 bar, V(II) is always close to 1, so that the water-gas shift is close to equilibrium; but this is not the case for 3 and 5 bar. Although the V(II) values decrease when $W/F^{\circ}_{CH_4}$ is decreased, extrapolation of the curves does not lead to the origin. Therefore, it is unlikely that CO_2 would be formed exclusively out of CO. Reaction schemes with a parallel contribution to the CO_2 formation are required.

A similar reasoning applied to the data on the reverse of the water-gas shift and methanation, indicates that among the six reactions involving carbon, five reactions (VII to XI) proceed to the right and could yield carbon. Even then, they would not significantly affect the mass balance, however. The process can be described on the basis of reactions I to III.

Reaction schemes

Among the large number of reaction schemes developed, only the two schemes which remained competitive to the very end of the model discrimination, Figures 7 and 8, are discussed here. In developing these schemes the following assumptions were made, based on our observations and information which is fairly well accepted in the literature:

1) H_2O reacts with surface nickel atoms, yielding adsorbed oxygen and gaseous hydrogen.

Table 2. Possible Reactions in Methane Steam Reforming

No.	Reactions	$-\Delta H_{298}$, kJ/mol
I	$CH_4 + H_2O = CO + 3H_2$	−206.1
II	$CO + H_2O = CO_2 + H_2$	+41.15
III	$CH_4 + 2H_2O = CO_2 + 4H_2$	−165.0
IV	$CH_4 + CO_2 = 2CO + 2H_2$	−247.3
V	$CH_4 + 3CO_2 = 4CO + 2H_2O$	−330.0
VI	$CH_4 = C + 2H_2$	−74.82
VII	$2CO = C + CO_2$	+173.3
VIII	$CO + H_2 = C + H_2O$	+131.3
IX	$CO_2 + 2H_2 = C + 2H_2O$	+90.13
X	$CH_4 + 2CO = 3C + 2H_2O$	+187.6
XI	$CH_4 + CO_2 = 2C + 2H_2O$	+ 15.3

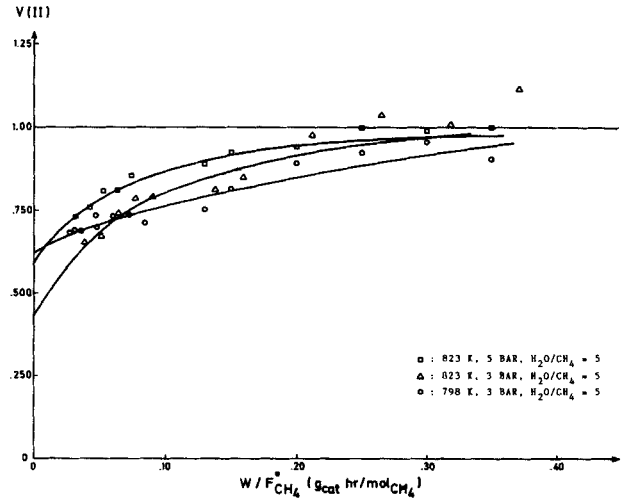

Figure 6. V(II) vs. space time, $W/F^{o}_{CH_4}$.

2) Methane is adsorbed on surface nickel atoms. The adsorbed methane either reacts with the adsorbed oxygen or is dissociated to form chemisorbed radicals, such as CH_3—L, CH_2—L, CH—L, and C—L.

3) The concentrations of the carbon-containing radicals, CH_3—L, CH_2—L, CH—L, and C—L, are much lower than the total concentration of the active sites.

4) The adsorbed oxygen and the carbon containing radicals react to form L—CH_2O, L—CHO, or L—CO, L—CO_2 (Menon et al., 1985).

5) The hydrogen formed is directly released into the gas phase and/or the gaseous hydrogen is in equilibrium with H—L or H_2—L.

6) All the reaction schemes are thought to have a step for reactions I, II and III with a rate potentially much slower than that of the other steps, so that it controls the overall reaction rate. It is the rate-determining step (RDS).

Scheme I contains the parallel formation of CO and CO_2 out of adsorbed CH_4 and the radicals derived from it. Scheme II includes mechanisms which consider parallel formation of CO and CO_2, out of CHO—L, a species which does not appear in Figure 7.

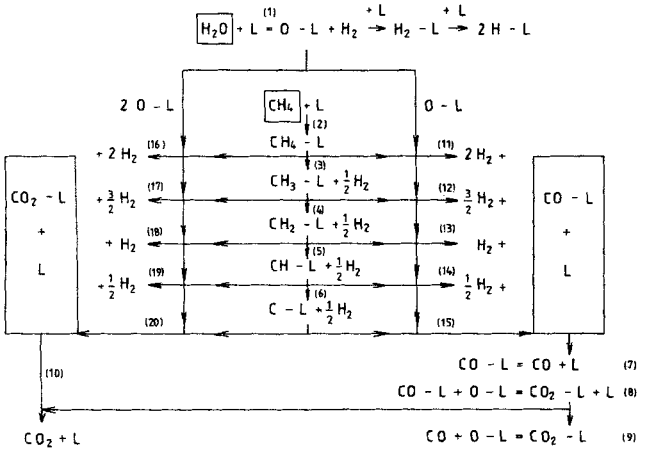

Figure 7. Reaction scheme I.

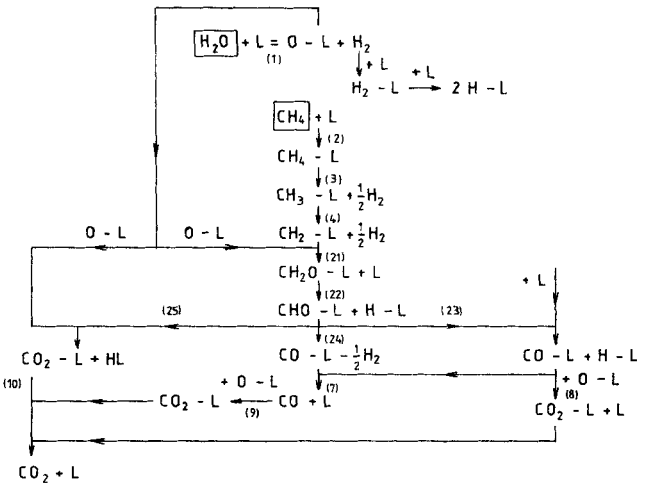

Figure 8. Reaction scheme II.

It follows from the thermodynamic analysis that reaction schemes generating all the CO_2 out of CO and those with CO and CO_2 formed directly from methane are not likely. Therefore, depending on the rate-determining steps, 21 sets of rate equations were generated out of the schemes in Figures 7 and 8.

These rate equations were derived in the way which is now classical for a single reaction. Rate equations were written for the rate-determining step of each of the three global reactions I, II and III, in terms of the concentrations of the adsorbed species. These concentrations were then eliminated by means of the Langmuir equilibrium relations and a balance on the active sites including those left vacant and those covered by adsorbed species. This yielded rate equations in terms of accessible gas-phase partial pressures and that contain a denominator resulting from the adsorption of reacting species (*viz.*, Eqs. 3). Since the three reactions are assumed to take place on the same active sites, the three rate equations have the same denominator.

Model Discrimination and Parameter Estimation

Methodology

Since the reactor was operated in the integral mode, parameter estimation was based on the minimization of the sum of weighted residual squares of the conversions and by means of the Marquardt routine. Parameter estimation for the multiresponse problem was based on the maximum likelihood concept. The details of the parameter estimation by the maximum likelihood method are described in Hosten and Froment (1975). The calculated conversions were obtained by integrating the set of continuity equations for the reference components. These equations are ordinary differential equations. They were integrated by the fourth-order Runge-Kutta routine. The continuity equations for CH_4 and CO_2 in steam reforming are as follows:

$$dx_{CH_4}/d(W/F^{o}_{CH_4}) = r_{CH_4}$$
$$dx_{CO_2}/d(W/F^{o}_{CH_4}) = r_{CO_2} \qquad (1)$$

with boundary conditions

$$\text{at } W/F^{o}_{CH_4} = 0, \quad x_{CH_4} = x_{CO_2} = 0$$

For the reverse of the water-gas shift and the methanation, the continuity equations are similar to those for steam reforming:

$$dx'_{CO_2}/d(W/F^o_{CO_2}) = r'_{CO_2}$$
$$dx'_{CH_4}/d(W/F^o_{CO_2}) = r'_{CH_4}$$

with boundary conditions at

$$W/F^o_{CO_2} = 0, \quad x'_{CO_2} = x'_{CH_4} = 0 \tag{2}$$

The reaction scheme leading to the retained set of rate equations and generated out of the detailed scheme of Figure 8, is shown in Table 3. This scheme is the detailed mechanistic expression of the following global triangular scheme (reactions I, II and III of Table 2):

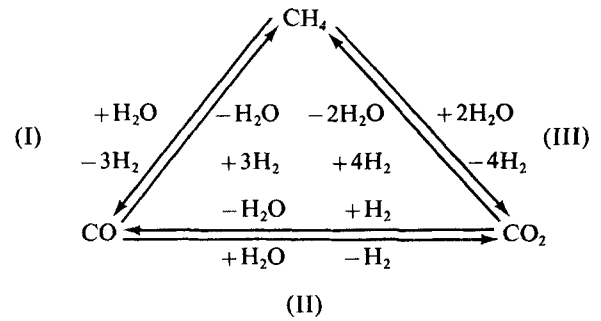

The corresponding rate equations are:

For reaction I of Table 3:

$$r_1 = \frac{k_1}{p_{H_2}^{2.5}}\left(p_{CH_4}p_{H_2O} - \frac{p_{H_2}^3 p_{CO}}{K_1}\right)\Big/(DEN)^2$$

For reaction II:

$$r_2 = \frac{k_2}{p_{H_2}}\left(p_{CO}p_{H_2O} - \frac{p_{H_2}p_{CO_2}}{K_2}\right)\Big/(DEN)^2 \tag{3}$$

For reaction III:

$$r_3 = \frac{k_3}{p_{H_2}^{3.5}}\left(p_{CH_4}p_{H_2O}^2 - \frac{p_{H_2}^4 p_{CO_2}}{K_3}\right)\Big/(DEN)^2$$

$$DEN = 1 + K_{CO}p_{CO} + K_{H_2}p_{H_2} + K_{CH_4}p_{CH_4} + K_{H_2O}p_{H_2O}/p_{H_2}$$

Reaction rates for the formation of CO and CO_2 and for the disappearance of methane in steam reforming are obtained from:

$$r_{CO} = r_1 - r_2$$
$$r_{CO_2} = r_2 + r_3$$
$$r_{CH_4} = r_1 + r_3 \tag{4}$$

Two of these rate equations are independent. These are the rate equations which were substituted into Eq. 1 for the data treatment of the steam reforming experiments.

Reaction rates for the disappearance of CO_2 and for the formation of CO and CH_4 in the reverse of the water-gas shift and methanation (CO_2 and H_2 as feed) are obtained from:

$$r_{CO} = r_1 - r_2$$
$$r'_{CO_2} = -(r_2 + r_3)$$
$$r'_{CH_4} = -(r_1 + r_3) \tag{5}$$

These are the rates which were substituted into Eq. 2.

The adequacy of the fit of each of the 21 sets of rate equations was tested by means of the F value, the significance of the parameters by means of the t value and 95% confidence interval of the parameter estimates. The F value is calculated by dividing the mean squares due to regression (the sum of squares of the predicted responses divided by the number of parameters) by the mean residual squares (the sum of residual squares divided by the degree of freedom of residuals, which is the number of experiments minus the number of parameters). The t value of a parameter estimate is the ratio of the parameter estimate minus zero and the standard deviation of that parameter. If a parameter is found to have a very small t value or a large confidence interval including zero, it is considered to have no significant contribution to the rate equations. Consequently, it may be deleted from the latter.

Table 3. Reaction Scheme and Corresponding Steps in Figure 8

H_2O	+ L	= O-L	+ H_2	(1)
CH_4	+ L	= CH_4-L		(2)
CH_4-L	+ L	= CH_3-L	+ H-L	(3)
CH_3-L	+ L	= CH_2-L	+ H-L	(4)
CH_2-L	+ O-L	= CH_2O-L	+ L	(21)
CH_2O-L	+ L	= CHO-L	+ H-L	(22)
CHO-L	+ L	= CO-L	+ H-L	(23) r.d.s.; r_1
CO-L	+ O-L	= CO_2-L	+ L	(8) r.d.s.; r_2
CHO-L	+ O-L	= CO_2-L	+ H-L	(25) r.d.s.; r_3
CO-L		= CO	+ L	(7)
CO_2-L		= CO_2	+ L	(10)
2H-L		= H_2-L	+ L	(1-bis)
H_2-L		= H_2	+ L	(1-bis)

Results

Five of the 21 sets of rate equations generated out of the reaction schemes of Figures 7 and 8 were rejected after the model discrimination and parameter estimation based on the experimental results of steam reforming. This procedure was insufficient to discriminate further, since the t values of some of the parameters were too small, possibly because of a too narrow investigated temperature range. The model discrimination and parameter estimation including the reverse of the water-gas shift and methanation experiments allowed 15 of the remaining 16 sets of rate equations to be rejected.

Since the partial pressures of CH_4 and H_2O were low in the experiments on the reverse of water-gas shift and methanation, the adsorption coefficients K_{CH_4} and K_{H_2O} could not be estimated significantly from these experiments. In the steam reforming experiments, the water-gas shift is very close to equilibrium so that k_2 cannot be estimated significantly at such conditions. The k_2 values were determined from the reverse water-gas shift and methanation data. Besides, for steam reforming conditions, the

Table 4. Parameter Estimates of the Final Model, Estimated per Temperature (Reference Conditions)

T(K)	k_1	k_2	k_3	K_{CO}	K_{H_2}	K_{CH_4}	K_{H_2O}	F
Reverse of Water–Gas Shift and Methanation								
573	$8.664\ 10^{-7}$	3.962	$1.965\ 10^{-7}$	417.1	0.2317	—	—	1,357
t	(4.27)	(4.92)	(5.07)	(6.40)	(3.49)			
598	$4.655\ 10^{-6}$	4.481	$6.627\ 10^{-7}$	104.4	0.1155	—	—	1,414
t	(6.72)	(8.60)	(7.39)	(9.73)	(3.19)			
623	$3.050\ 10^{-5}$	5.089	$5.149\ 10^{-6}$	59.90	0.1400	—	—	1,944
t	(8.63)	(10.4)	(13.23)	(17.0)	(3.83)			
648	$1.626\ 10^{-4}$	7.333	$2.541\ 10^{-5}$	32.35	0.09946	—	—	3,209
t	(12.6)	(13.4)	(9.27)	(13.1)	(3.54)			
673	$7.132\ 10^{-4}$	9.282	$1.457\ 10^{-4}$	23.6	−0.05641	—	—	2,627
t	(4.05)	(4.96)	(7.13)	(6.70)	(−0.845)			
Steam Reforming								
773	0.2088	—	−0.01216	—	—	0.3218	0.1300	8,123
t	(5.32)		(−1.50)			(6.12)	(1.65)	
798	0.5254	—	−0.00507	—	—	0.2174	0.1999	16,514
t	(5.65)		(−0.120)			(3.47)	(1.7)	
823	2.069	—	0.4452	—	—	0.4356	0.6412	19,338
t	(3.55)		(0.766)			(2.74)	(1.91)	

CO partial pressures are relatively low, while the K_{H_2} values are low, due to the high temperatures. The K_{CO} and K_{H_2} values were, therefore, calculated from the reverse water-gas shift and methanation data. No statistically significant values were obtained for K_{CO_2}, neither from the reverse of the water-gas shift, nor from the steam reforming experiments. This is why there is no term containing K_{CO_2} in the denominator of the set of rate equations (Eqs. 3).

The retained set of equations (Eqs. 3) is found to fit the experimental data well and the significant parameter estimates satisfy the Arrhenius equation and the van't Hoff equation, as shown in Table 4 and by the points in Figure 9. The k_3 values calculated from the steam-reforming data at 773 and 798 K are negative, but not significant. They are not shown in Figure 9.

The parameter estimation was then further implemented with all the data at all the temperatures together. To speed up the convergence of the minimization procedure, the rate and adsorption parameters were reparameterized according to Eqs. 6 and 7, with reference temperature T_r = 648 K for the k_i, K_{CO} and K_{H_2}, and 823 K for K_{CH_4} and K_{H_2O}.

$$k_i = k_{i,T_r} \exp\left[-\frac{E_i}{R}\left(\frac{1}{T}-\frac{1}{T_r}\right)\right] \quad i = 1, 2, 3 \tag{6}$$

$$K_j = K_{j,T_r} \exp\left[-\frac{\Delta H_j}{R}\left(\frac{1}{T}-\frac{1}{T_r}\right)\right] j = \mathrm{CO}, \mathrm{H_2}, \mathrm{CH_4}, \mathrm{H_2O} \tag{7}$$

The results are shown in Table 5 and Figure 9.

The t values of the activation energies E_1, E_2, and E_3 are high, meaning that the rate coefficients satisfy the Arrhenius equations. The adsorption enthalpies ΔH_{CO}, ΔH_{CH_4} and ΔH_{H_2} satisfy the van't Hoff equation, but not ΔH_{H_2O}, as evident from Figure 9.

The preexponential factors $A(k_i)$ and $A(K_j)$ can be calculated from the k_{i,T_r} and K_{j,T_r} and E_i and ΔH_j values by the Arrhenius equation and van't Hoff equation:

$$A(k_i) = k_{i,T} \exp\left(\frac{E_i}{RT}\right)$$

$$A(K_j) = K_{j,T} \exp\left(\frac{\Delta H_j}{RT}\right)$$

They are listed in Table 6.

The fit of the experimental data can be seen from the plotted experimental and calculated results, Figures 2 to 5. The curves in Figures 4 and 5 on reverse water-gas shift and methanation were obtained after multiplication of the rate parameters of Table 6 by 1.225, as explained earlier.

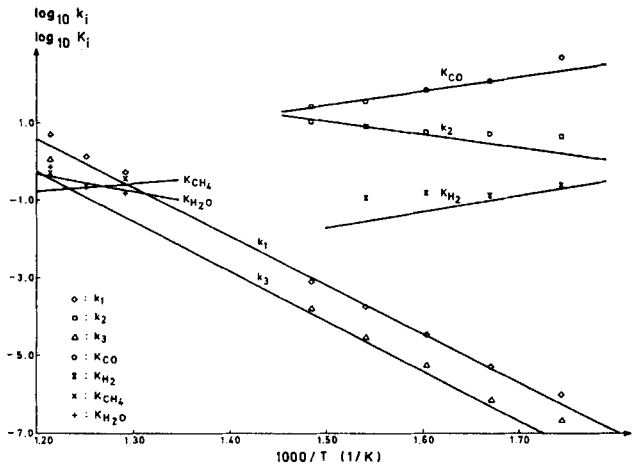

Figure 9. Temperature dependence of rate and adsorption parameters.
points: values estimated per temperature
lines: calculated from values in Tables 4 and 5

Parameters for the fresh catalyst

The steam reforming data were obtained with partially deactivated catalyst. In theory, the activity level of the fresh catalyst may be obtained by extrapolating the x_{CH_4} vs. time on stream curve in Figure 1 to $t = 0$. It can be seen from the plot that this is not too accurate, since it takes some time to stabilize the conditions. Deactivation is negligible under the conditioning for the

Table 5. Parameter Estimates for the Final Model: Simultaneous Regression of Data on Steam Reforming, Reverse of Water-Gas Shift, and Methanation at All Temperatures

	$k^{**}_{1,648}$	$k_{2,648}$	$k_{3,648}$	$K_{CO,648}$	$K_{H_2,648}$	$K^{**}_{CH_4,823}$	$K_{H_2O,823}$
	$1.842\ 10^{-4}$	7.558	$2.193\ 10^{-5}$	40.91	0.02960	0.1791	0.4152
t Value	(17.94)	(23.53)	(10.69)	(21.87)	(2.501)	(8.535)	(9.445)
UL^*	$2.05\ 10^{-4}$	8.200	$2.60\ 10^{-5}$	44.65	0.0533	0.2211	0.5032
LL^*	$1.64\ 10^{-4}$	6.915	$1.78\ 10^{-5}$	37.17	0.0059	0.1371	0.0317
	E_1	E_2	E_3	ΔH_{CO} (kJ/mol)	ΔH_{H_2}	ΔH_{CH_4}	ΔH_{H_2O}
	240.1	67.13	243.9	−70.65	−82.90	−38.28	88.68
t	(108.0)	(27.21)	(43.83)	(−23.47)	(−5.473)	(−4.403)	(23.97)
UL^*	244.5	72.06	255.0	−64.61	−52.61	−20.89	96.06
LL^*	235.7	62.19	232.7	−76.66	−113.2	−55.66	81.26

*UL = upper limit, LL = lower limit of approximate 95% confidence interval.
**648 and 823 are the values of the reference temperatures.

reverse of the water-gas shift and for methanation. Therefore, the initial activity was obtained from those experiments. After the temperature was reduced from 1,083 to 673 K, H_2 and CO_2 were fed at a molar ratio: $H_2/CO_2 = 1.0$. The pressure was set at 3 bar. Experiments at six different $W/F^o_{CO_2}$ values were performed at the above-mentioned conditions. The factor relating the rate coefficients for the initial activity level to those obtained with the deactivated catalyst and mentioned in Tables 5 and 6, was found by minimizing the sum of the squares of residuals of the data with fresh catalyst and those predicted by the model. This factor was found to be 2.246. All the reaction rate coefficients listed in Table 5 have to be multiplied by a factor of 2.246 when the rate equation and the parameters are to be used with fresh catalyst.

Thermodynamic consistency of the parameter estimates

Thermodynamics imposes the relation $\vec{E} - \overleftarrow{E} = \Delta H$. Since the activation energies for the forward and reverse reactions are positive.

$$E > \Delta H \tag{8}$$

Most authors, except for Rennhack and Heinisch (1972), De Deken et al. (1982), and Meyer and Köpsel (1981), obtained activation energies lower than 170 kJ/mol, the minimum value of the enthalpy changes of the steam reforming reactions I and III, which is in contradiction with Eq. 8. The estimates of the activation energies and enthalpy changes of reactions I, II and III are given in Table 7.

The adsorption constants have to satisfy a number of thermodynamic criteria (Boudart et al., 1967):

$$\text{i)}\ \Delta S^o_{j,a} < 0 \quad \text{or} \quad \exp(\Delta S^o_j/R) = A(K_j) < 1 \tag{9}$$

The preexponential factors of the adsorption constants, the $A(K_j)$ values, satisfy this rule:

$$A(K_{CO}) = 8.23\ 10^{-5} < 1,$$
$$A(K_{H_2}) = 6.13\ 10^{-9} < 1,$$
$$A(K_{CH_4}) = 6.65\ 10^{-4} < 1.$$

ii) For the nondissociative adsorptions, the following rule should be satisfied (Boudart et al., 1967):

$$-\Delta S^o_{j,a} < S^o_{j,g} \tag{10}$$

For CO, H_2, and CH_4, the $S^o_{i,g}$ values at 298 K are 198.5, 130.5, and 186.1 J/(mol · K), respectively. The criterion thus becomes:

$$\exp(\Delta S^o_{CO,a}/R) = A(K_{CO}) > \exp(-S^o_{CO,g}/R) = 4.7910^{-11}$$
$$\exp(\Delta S^o_{H_2,a}/R) = A(K_{H_2}) > \exp(-S^o_{H_2,g}/R) = 1.5110^{-7}$$
$$\exp(\Delta S^o_{CH_4,a}/R) = A(K_{CH_4}) > \exp(-S^o_{CH_4,g}/R) = 1.8810^{-10}$$

With the $A(K_{CO})$ and $A(K_{CH_4})$ values given under i), this criterion is satisfied for CO and CH_4 adsorption. The $A(K_{H_2})$ value is smaller than $1.51 \cdot 10^{-7}$.

iii) The third criterion is:

$$\Delta S^o_{j,a} \geq 0.0014\,\Delta H_{j,a} - 12.2 \tag{11a}$$

or

$$\ln A(K_j) = -\Delta S^o_{j,a}/R \leq (12.2 - 0.0014\,\Delta H_{j,a})/R \tag{11b}$$

Table 6. Preexponential Factors for Final Model*

$A(k_1)$	$A(k_2)$	$A(k_3)$	$A(K_{CO})$	$A(K_{H_2})$	$A(K_{CH_4})$	$A(K_{H_2O})$
$4.225\ 10^{15}$	$1.955\ 10^{6}$	$1.020\ 10^{15}$	$8.23\ 10^{-5}$	$6.12\ 10^{-9}$	$6.65\ 10^{-4}$	$1.77\ 10^{5}$

*Reference activity.

Table 7. Activation Energies and Changes in Reaction Enthalpy

Activation Energy (kJ/mol)					
E_1		E_2		E_3	
240.1		67.13		243.9	
Enthalpy Change (kJ/mol) of Reactions I to III					
948 K			298 K		
ΔH_1^o	ΔH_2^o	ΔH_3^o	ΔH_1^o	ΔH_2^o	ΔH_3^o
224.0	−37.3	187.5	206.1	−41.15	164.9

The parameter estimates also satisfy this criterion:

Component	$\ln A(K_j)$	$(12.2 - 0.0014\,\Delta H_{j,a})/R$
CO	−9.40	17.97
H_2	−18.90	17.87
CH_4	−7.32	7.763

iv) Usually, the absolute values of entropy changes for the nondissociative adsorption are higher than 42 J/mol · K. Since the $\Delta S_{j,a}^o$ values of CO, H_2 and CH_4 are 77.12, 157.0 and 60.81 J/mol · K, respectively, this rule is satisfied.

Discussion

The activation energies of reactions I and III are 240.1 and 243.9 kJ/mol. These values are very close to the activation energy obtained by Rennhack and Heinisch (1982) (247.9 kJ/mol) for methane disappearance and those obtained by Meyer and Köpsel (1981) (250.4 kJ/mol for reaction I and 205.8 kJ/mol for reaction III). Since Rennhack and Heinisch used nickel fibers as catalyst, no diffusional limitations existed in their study. The surface area of nickel fibers is also much smaller than that of a porous catalyst. Therefore, the heat absorbed by the reaction per unit volume of reactor is small enough to easily achieve isothermal conditions. Meyer and Köpsel (1981) used rather fine catalyst particles (0.25–0.63 mm) and the nickel content of their catalyst was rather low (6.62% Ni). These factors may diminish, if not eliminate, the effect of the internal diffusional limitations.

The majority of the authors, who used porous catalysts, obtained activation energies for reactions I and III smaller than the enthalpy changes, probably as a consequence of diffusional limitations or nonisothermal operation.

From Eqs. 3, it is clear that the predicted rates become infinite when the partial pressure of hydrogen is zero. Its origin can be traced back to the reaction mechanism shown in Table 3, in which it is assumed that the adsorption of hydrogen satisfies the equilibrium relation. This should not create a problem, though, in the application of these kinetic equations to the simulation of a reformer, since the feed generally contains some hydrogen or higher hydrocarbons which are very rapidly transformed into hydrogen and carbon monoxide.

In the simulation and design of industrial reactors, the intrinsic kinetic equations presented here have to be combined with the formulation of the diffusional limitations encountered when large catalyst particles are used. This aspect will be discussed in Part II of this paper that follows.

Notation

$A(k_i)$ = preexponential factor of rate coefficient, k_i
$A(K_j)$ = preexponential factor of adsorption constant, K_j
E_1, E_2, E_3 = activation energy of reactions I, II and III, kJ/mol
$F_{CH_4}^o, F_{CO_2}^o$ = molar feed rate of CH_4 and CO_2, kmol/h
ΔH = enthalpy change of reaction or adsorption, kJ/mol
K_1, K_3 = equilibrium constant of reactions I and III, bar^2
K_2 = equilibrium constant of reaction II
$K_{CH_4}, K_{CO}, K_{H_2}$ = adsorption constants for CH_4, CO and H_2, bar^{-1}
K_{H_2O} = dissociative adsorption constant of H_2O
k_1, k_3 = rate coefficient of reaction I and III, kmol · $bar^{1/2}$/(kg cat · h)
k_2 = rate coefficient of reaction II, kmol/(kg cat · h · bar)
P = total pressure, bar
p_j = partial pressure of component j, bar
R = gas constant, kJ/kmol
r_1, r_2, r_3 = rates of reactions I, II and III, kmol/(kg cat · h)
r_{CH_4} = rate of methane disappearance in steam reforming, kmol CH_4/(kg cat · h)
r'_{CH_4} = rate of methane formation in the reverse of water-gas shift and methanation, id
r_{CO} = rate of CO formation in steam reforming of methane, kmol CO/(kg cat · h)
r'_{CO} = rate of CO formation in the reverse of water-gas shift and methanation, id
r_{CO_2} = rate of CO_2 formation in steam reforming, kmol CO_2/(kg cat · h)
r'_{CO_2} = rate of CO_2 disappearance in the reverse of water-gas shift and methanation, id
$S_{j,g}^o$ = standard entropy of gas component j, kJ/(kmol · K)
$S_{j,a}^o$ = entropy of species j in the adsorbed state, kJ/(kmol · K)
ΔS = entropy change, kJ/(kmol · K)
T = temperature, K
T_r = reference temperature used in reparameterization, K
$V(i) = (\Pi/j \cdot p_j^{\nu_j})_i/K_i$ where ν_j is the stoichiometric coefficient of component j in reaction i
W = weight of catalyst, kg
x_{CH_4} = total methane conversion in steam reforming, kmol CH_4/kmol CH_4 fed
x'_{CH_4} = conversion of CO_2 into methane in the reverse of water-gas shift and methanation, kmol CH_4/kmol CO_2 fed
x_{CO} = conversion of methane into CO in steam reforming, kmol CO/kmol CH_4 fed
x'_{CO_2} = total CO_2 conversion in the reverse water-gas shift and methanation, kmol CO_2/kmol CO_2 fed
x_{CO_2} = conversion of methane into CO_2 in steam reforming, kmol CO_2/kmol CH_4 fed

Acknowledgment

J. Xu is grateful to Commissariaat-Generaal voor de Internationale Culturele Samenwerking van de Vlaamse Gemeenschap, Belgium, for the financial support during his Ph.D. work.

Literature Cited

Akers, W. W., and D. P. Camp, "Kinetics of the Methane-Steam Reaction," *AIChE J.*, **1**(4), 471 (1955).

Allen, D. W., E. R. Gerhard, and M. R. Likins, "Kinetics of the Methane-Steam Reaction," *Ind. Eng. Chem. P. D. D.*, **14**(3), 256 (1975).

Boudart, M., D. E. Mears, and M. A. Vannice, "Kinetics of Heterogeneous Catalytic Reactions," Congrès International Chimie Industrielle, Compte-Rendu 36, Industrie Chimique Belge, **32** (I), 281 (1967).

De Deken, J., E. F. Devos, and G. F. Froment, "Steam Reforming of

Natural Gas: Intrinsic Kinetics, Diffusional Influences, and Reactor Design," *Chemical Reaction Engineering, ACS Symp. Ser.*, 196, Boston (1982).
Hosten, L. H., and G. F. Froment, "Parameter Estimation in Multi-Response Models," *Periodica Polytechnica*, **19**, (1–2) (1975).
Menon, P. G., J. De Deken, and G. F. Froment, "Formaldehyde as an Intermediate in the Steam Reforming of Methane," *J. Catal.*, **95**, 313 (1985).
Meyer, B., and R. Köpsel, "Reaktionskinetik der Methanwasserdampf-Knovertierung am Katalysator GIAP3-6N," Veb Deutscher Verlag fur Grundstoff-Industrie, Leipzig, from Reference II (1981).
Rennhack, R., and R. Heinisch, "Kinetische Untersuchung der Reaktion Zwischen Methan und Wasserdampf an Nickel-Oberflächen," *Erdöl und Kohle-Erdgas-Petrochemie Vereinigt mit Brennstoff-Chemie*, **1**, 22, Jahrgang, Germany (1972).
Ross, J. R. H., and M. C. F. Steel, "Mechanism of the Steam Reforming of Methane Over a Coprecipitated Nickel-Alumina Catalyst," *J. Chem. Soc., Farad. Trans.*, **1**(1), 10 (1973).
Rostrup-Nielsen, J. R., "Activity of Nickel Catalysts for Steam Reforming of Hydrocarbons," *J. Catal.*, **31**, 173 (1973).

Manuscript received Feb. 29, 1988, and revision received Sept. 2, 1988.